UNIVERSITY
OF TRENTO

Department of Physics

Bachelor's Degree in Physics

Path Integral Monte Carlo

Supervisor:

Alessandro Roggero

Student:

Federico Periotto

Academic year 2023/2024

Contents

Abstract

The purpose of this thesis is to show how Path Integral Monte Carlo (PIMC) simulations can be used to compute the quantum properties of a system. More specifically, the thesis starts with an introduction to Feynman's path integrals and their use in Monte Carlo simulations giving rise to the PIMC theory. Two different algorithms for sampling new paths are introduced: one that follows the classic rule of random displacement and one that aims to improve it. We introduce the computation of path integrals on a lattice, taking the one-dimensional quantum harmonic oscillator as an example and then adding an anharmonic contribution treated as a perturbation. We can use the system's action in PIMC simulations to bring it to equilibrium and calculate the physical quantities we are interested in, we focus on the internal energy at different temperatures. The values obtained from these simulations often exhibit autocorrelation, we see a method to estimate a better standard deviation on the results obtained.

Chapter 1

Background

1.1 Path integral

Let us consider a system with Hamiltonian H. Energy eigenfunctions and eigenvalues are respectively $|i\rangle$ and E_i, such that

$$H|i\rangle = E_i|i\rangle.$$

We will work in the canonical ensemble where the system has fixed volume V, number of particles N, and temperature T. The equilibrium properties of the system are determined by the density matrix:

$$\rho = e^{-\beta\hat{H}} = \sum_n e^{-\beta E_i}|i\rangle\langle i| \quad \text{with } \beta = \frac{1}{k_B T}$$

The state $|i\rangle$ is occupied with probability proportional to $e^{-\beta E_i}$. The equilibrium value of an operator O is

$$\langle O\rangle = \frac{Tr\left[\rho O\right]}{Z} = \frac{1}{Z}\sum_i \langle i|O|i\rangle e^{-\beta E_i},$$

$$Z = Tr[\rho] = \sum_i e^{-\beta E_i}$$

where Z is the partition function.
In position-space, the density matrix is:

$$\rho(\mathbf{R},\mathbf{R}';\beta) = \langle \mathbf{R}|e^{-\beta H}|\mathbf{R}'\rangle = \sum_i \langle \mathbf{R}|i\rangle\langle i|\mathbf{R}'\rangle e^{-\beta E_i} = \sum_i \Psi_i(\mathbf{R})\Psi_i^*(\mathbf{R}')e^{-\beta E_i}.$$

Where, $\mathbf{R} = (\mathbf{R}_1,\ldots,\mathbf{R}_N)$ are the coordinates of the N particles in D dimensions.
In the position representation, the expectation of O becomes

$$\langle O\rangle = \frac{1}{Z}\int d\mathbf{R}\, d\mathbf{R}'\langle \mathbf{R}|e^{-\beta H}|\mathbf{R}'\rangle\langle \mathbf{R}'|O|\mathbf{R}\rangle = \frac{1}{Z}\int d\mathbf{R}d\mathbf{R}'\rho(\mathbf{R},\mathbf{R}',\beta)\langle \mathbf{R}'|O|\mathbf{R}\rangle$$

And if O is diagonal

$$\langle O\rangle = \frac{1}{Z}\int d\mathbf{R}\, d\mathbf{R}'\rho(\mathbf{R},\mathbf{R}',\beta)O(\mathbf{R})\delta(\mathbf{R}-\mathbf{R}') = \frac{1}{Z}\int d\mathbf{R}\rho(\mathbf{R},\beta)O(\mathbf{R}) \tag{1.1}$$

We can also rewrite the density matrix as the product of multiple density matrices in the following way:

$$e^{-(\beta_1+\beta_2)H} = e^{-\beta_1 H} e^{-\beta_2 H},$$

Hence

$$\rho(\mathbf{R}_1, \mathbf{R}_3; \beta_1+\beta_2) = \int d\mathbf{R}_2 \langle \mathbf{R}_1 | e^{-\beta_1 H} | \mathbf{R}_2 \rangle \langle \mathbf{R}_2 | e^{-\beta_2 H} | \mathbf{R}_3 \rangle = \int d\mathbf{R}_2 \rho(\mathbf{R}_1, \mathbf{R}_2; \beta_1) \rho(\mathbf{R}_2, \mathbf{R}_3; \beta_2)$$

The process can be iterated M times:

$$e^{-\beta H} = \left(e^{-\tau H}\right)^M \quad \text{where} \quad \tau = \frac{\beta}{M},$$

yielding

$$\begin{aligned} \rho(\mathbf{R}_0, \mathbf{R}_M; \beta) &= \int d\mathbf{R}_1 \dots d\mathbf{R}_{M-1} \langle \mathbf{R}_0 | e^{-\tau H} | \mathbf{R}_1 \rangle \langle \mathbf{R}_1 | e^{-\tau H} | \mathbf{R}_2 \rangle \cdots \langle \mathbf{R}_{M-1} | e^{-\tau H} | \mathbf{R}_M \rangle \\ &= \int d\mathbf{R}_1 \dots d\mathbf{R}_{M-1} \rho(\mathbf{R}_0, \mathbf{R}_1; \tau) \dots \rho(\mathbf{R}_{M-1}, \mathbf{R}_M; \tau) \end{aligned} \tag{1.2}$$

This result is exact for any $M \geq 1$. The logic is that for sufficiently large values of M, $\tau = \frac{\beta}{M}$ corresponds to the highest temperature MT. This allows us to derive valid and sufficiently accurate approximations for the density matrix $\rho(\mathbf{R}_0, \mathbf{R}_M; \beta)$ by treating the $\rho(\mathbf{R}_i, \mathbf{R}_{i+1}; \tau)$ as classical density matrices. Several approximation methods have been introduced over the years.

1.1.1 Primitive Approximation

In general, the Hamiltonian is written as

$$H = \mathcal{T} + V$$

where $\mathcal{T}$ and V are the kinetic and the potential energy. From this, we can treat the exponential as follows

$$\begin{aligned} e^{-\tau H} &= e^{-\tau(\mathcal{T}+V)} = e^{-\tau \mathcal{T}} e^{-\tau \mathcal{V}} e^{+\tau^2 \frac{[\mathcal{T},\mathcal{V}]}{2}} + O(\tau^3) \\ &= e^{-\tau \mathcal{T}} e^{-\tau \mathcal{V}} + \frac{\tau^2}{2}[\mathcal{T}, \mathcal{V}] + O(\tau^3) = e^{-\tau \mathcal{T}} e^{-\tau \mathcal{V}} + O(\tau^2) \end{aligned} \tag{1.3}$$

if τ is small one can neglect the contribution of τ^2 and get the approximate result known as the *primitive approximation*:

$$e^{-\tau(\mathcal{T}+\mathcal{V})} \simeq e^{-\tau \mathcal{T}} e^{-\tau \mathcal{V}}.$$

Since the three operators $\mathcal{T}$, V and $\mathcal{T}+V$ are self-adjoint, Trotter's formula is valid:

$$e^{-\beta(\mathcal{T}+V)} = \lim_{M \to \infty} \left(e^{-\frac{\beta}{M}\mathcal{T}} e^{-\frac{\beta}{M} V} \right)^M$$

By using the primitive approximation one can write

$$\rho(\mathbf{R}_0, \mathbf{R}_2; \tau) = \int d\mathbf{R}' \langle \mathbf{R}_0 | e^{-\tau \mathcal{T}} | \mathbf{R}' \rangle \langle \mathbf{R}' | e^{-\tau V} | \mathbf{R}_2 \rangle$$

and evaluate the kinetic and the potential density matrices separately.
Since the potential energy is diagonal in the coordinate representation

$$\langle \mathbf{R}_1 | e^{-\tau V} | \mathbf{R}_2 \rangle = e^{-\frac{\tau}{2}(V(\mathbf{R}_1)+V(\mathbf{R}_2))} \delta(\mathbf{R}_1 - \mathbf{R}_2) = e^{-\tau V(\mathbf{R}_1)} \delta(\mathbf{R}_2 - \mathbf{R}_1)$$

The kinetic matrix can be evaluated using eigenfunction expansion of $\mathcal{T}$. In this thesis, we consider the case of distinguishable particles in a D-dimensional hypercube of side L with periodic boundary conditions.
The energies and eigenfunctions are

$$E_n = \frac{\hbar^2}{2m} K_n^2, \quad \langle \mathbf{R} | \Psi_n \rangle = \frac{1}{\sqrt{L^{DN}}} e^{i \mathbf{K}_n \cdot \mathbf{R}},$$

where $\mathbf{K}_n = \frac{2\pi}{L}\mathbf{n}$ and $\mathbf{n}$ a $DN-$dimensional integer vector.
The kinetic energy operator is given by

$$T = -\frac{\hbar^2}{2m} \sum_{i=1}^{N} \nabla_i^2$$

$$\langle \mathbf{R}_1 | e^{-\beta \mathcal{T}} | \mathbf{R}_2 \rangle = \sum_n \frac{1}{L^{DN}} e^{-i \mathbf{K}_n \cdot (\mathbf{R}_1 - \mathbf{R}_2)} e^{-\beta \frac{\hbar^2}{2m} K_n^2}.$$

The sum can be performed in the limit of a large box by transforming it into an integral and yielding after Gaussian integration.

$$\langle \mathbf{R}_1 | e^{-\beta \mathcal{T}} | \mathbf{R}_2 \rangle = \left(\frac{2\pi\hbar^2\beta}{m} \right)^{-DN/2} \exp\left(-\frac{(\mathbf{R}_1 - \mathbf{R}_2)^2}{2\hbar^2\beta/m} \right),$$

holding provided that $\lambda_T \ll L$ where $\lambda_T = \frac{\hbar^2\beta}{2m}$ is the thermal wavelength.
As a result, the density matrix for the interacting system can be written in this form

$$\begin{aligned} \rho(\mathbf{R}_0, \mathbf{R}_M; \beta) &= \int d\mathbf{R}_1 \dots d\mathbf{R}_{M-1} (4\pi\lambda\tau)^{-\frac{DNM}{2}} \exp\left(-\sum_{k=1}^{M} \left[\frac{(\mathbf{R}_{k-1} - \mathbf{R}_k)^2}{4\lambda\tau} + \tau V(\tilde{\mathbf{R}}_k) \right] \right) = \\ &= \int d\mathbf{R}_1 \dots d\mathbf{R}_{M-1} \exp\left(-\sum_{k=1}^{M} S_k \right) \end{aligned} \tag{1.4}$$

where $\lambda = \frac{\hbar^2}{2m}$ and S_k is the action of the $k-$th link and it is defined as:

$$\begin{aligned} S_k &= S(\mathbf{R}_{k-1}, \mathbf{R}_k; \tau) = -ln[\rho(\mathbf{R}_{k-1}, \mathbf{R}_k; \tau)] = \\ &= \frac{dN}{2} \log(4\pi\lambda\tau) + \frac{(\mathbf{R}_{k+1} - \mathbf{R}_k)^2}{4\lambda\tau} + \tau V(\tilde{\mathbf{R}}_k) \end{aligned} \tag{1.5}$$

This is the path integral. We can define $\tau = \beta/M$ as the *time step* and the single $\mathbf{R}_k$ is referred to the $k-th$ time slice. $\tilde{\mathbf{R}}_k$ represents the $3N$ position of the N particles: $\mathbf{R}_k = \{\mathbf{R}_{1,k}, \dots, \mathbf{R}_{N,k}\}$ and $\mathbf{R}_{i,k}$, a bead, in the position of the i-th particle in the k-th time slice. The path is the sequence of points $\{\mathbf{R}_0, \dots, \mathbf{R}_M\}$, and the time associated with the point $\mathbf{R}_k$ is represented as $t_k = k\tau$.

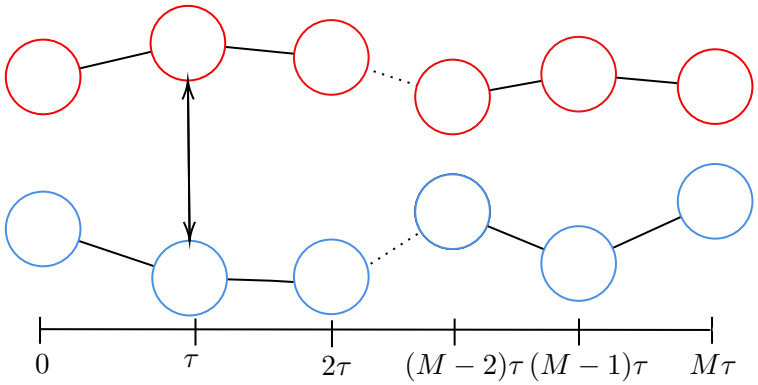

Figure 1.1: A useful way to depict particles is through world lines in imaginary time τ. The interactions between particles are within beads at the same time slice.

We can map the quantum system above to a classical polymer system. Considering Eq. 1.4, we can see that the exponential is the canonical potential summed with a term that has the same form as the potential for a set of particles $\vec{\mathbf{R}} = \{\mathbf{R}_k\}_{k=1}^{M}$ where each particle $\mathbf{R}_k$ is coupled to its closest neighbors $\mathbf{R}_{k-1}$ and $\mathbf{R}_{k+1}$ by springs. So the particles can be represented by M-particle polymer necklaces by making $\mathbf{R}_0$ coincide with $\mathbf{R}_M$. This necklace represents the same particle in successive time slices and the average extension of a polymer is determined by the thermal wavelength λ_T.

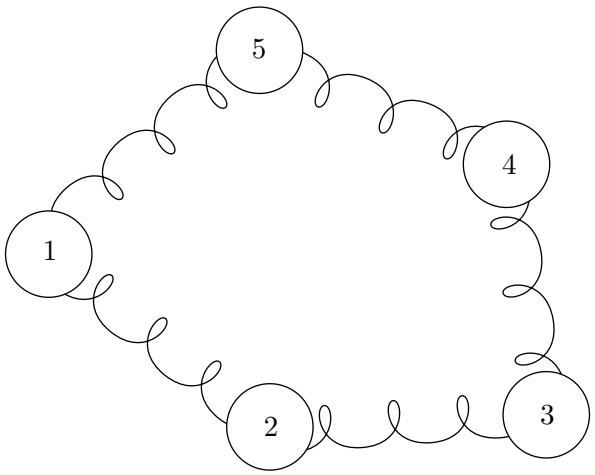

Figure 1.2: Example of a two-dimensional quantum particle in the classical view. The spring between the beads represents the elastic term obtained in the exponential and it is the kinetic potential between different times for two consecutive beads of the same particle.

All the approximations made on these pages are controllable. The shortcoming of having an explicit expression for the density matrix is additional integrations. Using simulative methods these multidimensional integrals can be treated accurately.

1.2 Path Integral Monte Carlo Method

By placing $\mathbf{R} \coloneqq \mathbf{R}_0 \equiv \mathbf{R}_M$ in the path-integral and substituting it in Eq. 1.1 one have:

$$\begin{aligned}\langle O \rangle &= \frac{1}{Z}\int d\mathbf{R}\rho(\mathbf{R},\beta)O(\mathbf{R}) = \int d\mathbf{R}\int d\mathbf{R}_1\dots d\mathbf{R}_{M-1}\frac{\exp\left(-\sum_{k=1}^{M}S_k\right)}{Z}O(\mathbf{R}) = \\ &= \int d\mathbf{R}\int d\mathbf{R}_1\dots d\mathbf{R}_{M-1}O(\mathbf{R})P(\{\mathbf{R},\mathbf{R}_1,\dots,\mathbf{R}_{M-1}\},\beta),\end{aligned} \tag{1.6}$$

where $P(\vec{\mathbf{R}})$ corresponds to the probability of a given configuration of the set of polymers $\vec{\mathbf{R}} = \{\mathbf{R},\mathbf{R}_1,\dots,\mathbf{R}_{M-1}\}$:

$$P(\vec{\mathbf{R}};\beta) = \frac{\prod_{k=1}^{M}\rho(\mathbf{R}_k,\mathbf{R}_{k-1};\beta)}{Z} = \frac{\exp\left(-\sum_{k=1}^{M}S_k\right)}{Z} \tag{1.7}$$

We went from an integral in $DN-$dimensions to one in DNM. Yet having introduced a probability distribution we can solve it stochastically by sampling it. We use the $M(RT)^2$ algorithm, this method can be used for virtually any distribution and any dimensionality. The disadvantage is that it is exact only in an asymptotic limit and tends to produce autocorrelated variables.
It is important to note that, in this distribution, the points along the path are linked together by elastic terms, which can cause simple simulation techniques to converge slowly. However, classical isomorphism can still be employed, and several simulation techniques can be utilized to study the dynamics.
We consider the system in configuration $\vec{\mathbf{X}} = \{\mathbf{R}_1,\dots,\mathbf{R}_M\}$. The kinematics of the system is a stochastic transition that governs the evolution of the system arriving, for example, at point $\vec{\mathbf{Y}} = \{\mathbf{R}'_1,\dots,\mathbf{R}'_M\}$. We write the transition probability as

$$K(\vec{\mathbf{X}} \to \vec{\mathbf{Y}}) = K(\vec{\mathbf{Y}}|\vec{\mathbf{X}})$$

Assuming all transitions to be ergodic the distribution converges to the unique equilibrium state. A transition is ergodic if it is possible to access any given state in a finite number of states.
The physical system is said to reach equilibrium when it becomes stationary and thus satisfies *detailed balance*:

$$P(\vec{\mathbf{X}})K(\vec{\mathbf{X}}|Y) = P(\vec{\mathbf{Y}})K(\vec{\mathbf{Y}}|\vec{\mathbf{X}})$$

Now the transition probability is split as:

$$K(\vec{\mathbf{X}}|\vec{\mathbf{Y}}) = T(\vec{\mathbf{X}}|\vec{\mathbf{Y}})A(\vec{\mathbf{X}}|\vec{\mathbf{Y}})$$

where $T(X|Y)$ is an *a priori* sampling distribution and $A(X|Y)$ is an acceptance probability. The trial moves are accepted or rejected according to:

$$A(\vec{\mathbf{Y}}|\vec{\mathbf{X}}) = \min\left[1, q(\vec{\mathbf{Y}}|\vec{\mathbf{X}})\right] \quad \text{with} \quad q(\vec{\mathbf{Y}}|\vec{\mathbf{X}}) = \frac{T(\vec{\mathbf{X}}|\vec{\mathbf{Y}})P(\vec{\mathbf{Y}})}{T(\vec{\mathbf{Y}}|\vec{\mathbf{X}})P(\vec{\mathbf{X}})} \tag{1.8}$$

This translates into the points reported in the following. Given $\vec{\mathbf{X}}$, we sample $\vec{\mathbf{Y}}'$ using the $q(\vec{\mathbf{Y}}'|\vec{\mathbf{X}})$ and:

- if $q(\vec{\mathbf{Y}}'|\vec{\mathbf{X}}) > 1$ we accept the move and $\vec{\mathbf{Y}} = \vec{\mathbf{Y}}'$;
- if $q(\vec{\mathbf{Y}}'|\vec{\mathbf{X}}) < 1$ we take a random number r between 0 and 1 and we accept if $q(\vec{\mathbf{Y}}'|\vec{\mathbf{X}}) > r$ otherwise $\vec{\mathbf{Y}} = \vec{\mathbf{X}}$.

At this point, it is necessary to choose the sampling distribution. We opted for bead-by-bead sampling, first moving them in random motion within an interval and then concerning Gaussians centered at favorable points.

1.2.1 Classic method: random movements

We take $T(\vec{\mathbf{X}}|\vec{\mathbf{Y}})$ uniform in an interval $\left[-\frac{\Delta}{2}, \frac{\Delta}{2}\right]$. With this choice we have $T(\vec{\mathbf{X}}|\vec{\mathbf{Y}}) = T(\vec{\mathbf{Y}}|\vec{\mathbf{X}})$ so that:

$$q(\vec{\mathbf{Y}}|\vec{\mathbf{X}}) = \frac{P(\vec{\mathbf{Y}})}{P(\vec{\mathbf{X}})}$$

The proposed move is like this:

$$\vec{\mathbf{Y}}' = \vec{\mathbf{X}} + \Delta\left(r - \frac{1}{2}\right) \quad \text{with } r \text{ uniform distributed in } [0,1]$$

Specifically given the M beads we take a random one and move it keeping the others fixed.

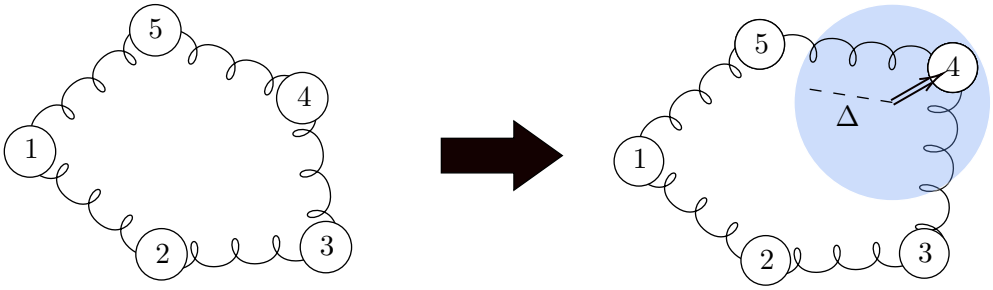

Figure 1.3: Example of random displacement for bead-by-bead sampling

1.2.2 Smarter method: Brownian bridge

Instead of proceeding to a random shift within a radius Δ we decide to change the sampling type and in particular change the *a priori* sampling distribution. We still operate with a single-slice movement (i.e., bead-by-bead sampling), we still randomly choose the bead to be moved, but once we choose the $k-$th bead the new position we assign to it does not depend on the old position but will be given by a Gaussian distribution (with $\sigma^2 = f(\beta, M)$) centered in $\overline{\mathbf{R}}_k = \frac{\mathbf{R}_{k+1}+\mathbf{R}_{k-1}}{2}$. The *a priori* distributions will then be given by:

$$T(\vec{\mathbf{R}} \to \vec{\mathbf{R}}') = \frac{1}{\sqrt{2\pi\sigma^2}} \exp\left(-\frac{(\mathbf{R}_k - \overline{\mathbf{R}}_k)^2}{2\sigma^2}\right),$$

$$T(\vec{\mathbf{R}}' \to \vec{\mathbf{R}}) = \frac{1}{\sqrt{2\pi\sigma^2}} \exp\left(-\frac{(\mathbf{R}'_k - \overline{\mathbf{R}}_k)^2}{2\sigma^2}\right).$$

In this approach, the movement of each bead is guided by a Brownian Bridge, a stochastic process that models the bead's position by considering its neighbors.

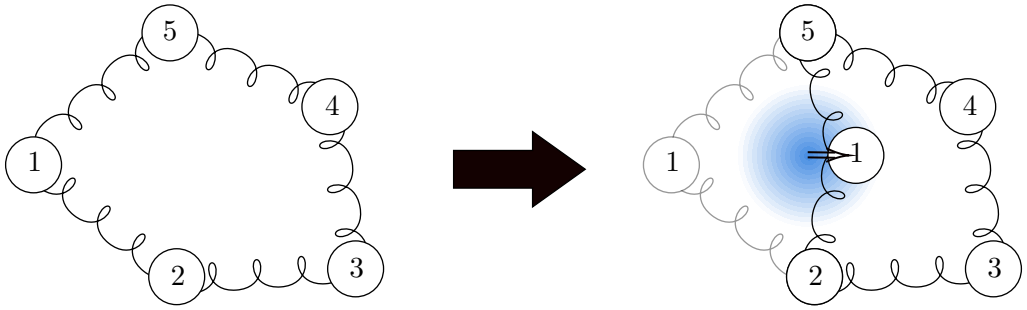

Figure 1.4: Example of gaussian displacement for bead-by-bead sampling

After the bead has been displaced, the action of the new position is compared with the acceptance criterion

$$A(\vec{\mathbf{R}} \to \vec{\mathbf{R}}') = \min\left[1, \frac{T(\vec{\mathbf{R}}' \to \vec{\mathbf{R}}) \exp\left(-\sum_{\mu=1}^{M} S'_\mu\right)}{T(\vec{\mathbf{R}} \to \vec{\mathbf{R}}') \exp\left(-\sum_{\mu=1}^{M} S_\mu\right)}\right].$$

We can develop the ratio in a way that results in a more intelligent value of the acceptance:

$$\frac{T(\vec{\mathbf{R}}' \to \vec{\mathbf{R}}) \exp\left(-\sum_{\mu=1}^{M} S'_\mu\right)}{T(\vec{\mathbf{R}} \to \vec{\mathbf{R}}') \exp\left(-\sum_{\mu=1}^{M} S_\mu\right)} = \exp\left(-\frac{(\mathbf{R}'_k - \overline{\mathbf{R}}_k)^2}{2\sigma^2} + \frac{(\mathbf{R}_k - \overline{\mathbf{R}}_k)^2}{2\sigma^2}\right) \times$$

$$\times \exp\left(\frac{\sum_{\nu}^{M}(\mathbf{R}_\mu - \mathbf{R}_{\mu-1})^2 - \sum_{\mu}^{M}(\mathbf{R}'_\mu - \mathbf{R}'_{\mu-1})^2}{4\lambda\tau}\right) \times \exp\left(-\tau\left[V(\mathbf{R}'_k) - V(\mathbf{R}_k)\right]\right).$$

The middle exponential can be simplified as

$$\exp\left(\frac{\sum_{\mu}^{M}(\mathbf{R}_\mu - \mathbf{R}_{\mu-1})^2 - \sum_{\mu}^{M}(\mathbf{R}'_\mu - \mathbf{R}'_{\mu-1})^2}{4\lambda\tau}\right) =$$

$$= \exp\left(\frac{\sum_{\mu}^{M}\left[\mathbf{R}_\mu^2 - 2\mathbf{R}_\mu\mathbf{R}_{\mu-1} + \mathbf{R}_{\mu-1}^2 - \mathbf{R}_\mu'^2 + 2\mathbf{R}'_\mu\mathbf{R}'_{\mu-1} - \mathbf{R}'^2_{\mu-1}\right]}{4\lambda\tau}\right) =$$

$$= \exp\left(\frac{\mathbf{R}_k^2 - 2\mathbf{R}_k\overline{\mathbf{R}}_k - \mathbf{R}_k'^2 + 2\mathbf{R}'_k\overline{R}_k}{2\lambda\tau}\right) = \exp\left(\frac{(\mathbf{R}'_k - \overline{\mathbf{R}}_k)^2 - (\mathbf{R}_k - \overline{\mathbf{R}}_k)^2}{2\lambda\tau}\right).$$

Setting the variance of $T(\vec{\mathbf{R}} \to \vec{\mathbf{R}}')$ to $\sigma^2 = \lambda\tau = \frac{\hbar^2\beta}{2mM}$ gives the simple expression for the acceptance probability

$$A(\vec{\mathbf{R}} \to \vec{\mathbf{R}}') = \min\left[1, e^{-\tau(V(\mathbf{R}'_k) - V(\mathbf{R}_k))}\right].$$

It is then possible to use only the potential of the bead before and after displacement provided that the Gaussian is centered in the middle of the neighboring beads and with the variance fixed by the law just written.

Chapter 2

Monte Carlo Simulation for quantum oscillator

2.1 The Harmonic Oscillator

The Hamiltonian of the harmonic oscillator is given by

$$H = \mathcal{T} + \mathcal{V} = \frac{p^2}{2m} + \frac{1}{2}m\omega^2 x^2$$

In this section, we consider both a classical harmonic oscillator following the Boltzmann distribution and a quantum harmonic oscillator studied using path-integral theory.
In the following pages we use natural units so $k_B = \hbar = 1$. We also fix $m = 1kg$ and $\omega = \delta\omega\tilde{\omega}$ with $\tilde{\omega} = 1\frac{rad}{s}$.
We also deal with one-dimensional single-particle systems so $D = 1$, $N = 1$, and the M bead system coordinates are $R_1, \ldots, R_M$.

2.1.1 Classical Harmonic Oscillator

For the classical harmonic oscillator deriving $\langle\mathcal{T}\rangle$ and $\langle V\rangle$ separately, assuming that the moment $\mathbf{p}$ is isotropic and uniformly distributed, we obtain:

$$\langle\mathcal{V}\rangle = \frac{\int V e^{-\beta H}\, dp\, dx}{\int e^{-\beta H}\, dp\, dx} = \frac{1}{2}m\omega^2 \frac{\int x^2 e^{-\beta\frac{1}{2}m\omega^2x^2}\, dx \int e^{-\beta\frac{p^2}{2m}}\, dp}{\int e^{-\beta\frac{1}{2}m\omega^2x^2}\, dx \int e^{-\beta\frac{p^2}{2m}}\, dp} =$$
$$= \frac{1}{2}m\omega^2 \frac{\int x^2 e^{-\beta\frac{1}{2}m\omega^2x^2} dx}{\int e^{-\beta\frac{1}{2}m\omega^2x^2}} = \frac{1}{\beta}\frac{\int x'^2 e^{-x'^2} dx'}{\int e^{-x'^2} dx'} = \frac{1}{2\beta} = \frac{1}{2}k_BT.$$

Similarly:

$$\langle\mathcal{T}\rangle = \frac{\int T e^{-\beta H}\, dp\, dx}{\int e^{-\beta H}\, dp\, dx} = \frac{1}{2}k_BT$$

Hence as expected from the virial theorem the average internal energy is

$$E_{cl} = k_BT = \frac{1}{\beta} \tag{2.1}$$

It can be seen that it is independent of the characteristic quantities of the harmonic oscillator. We show the trend in Fig. 2.1.

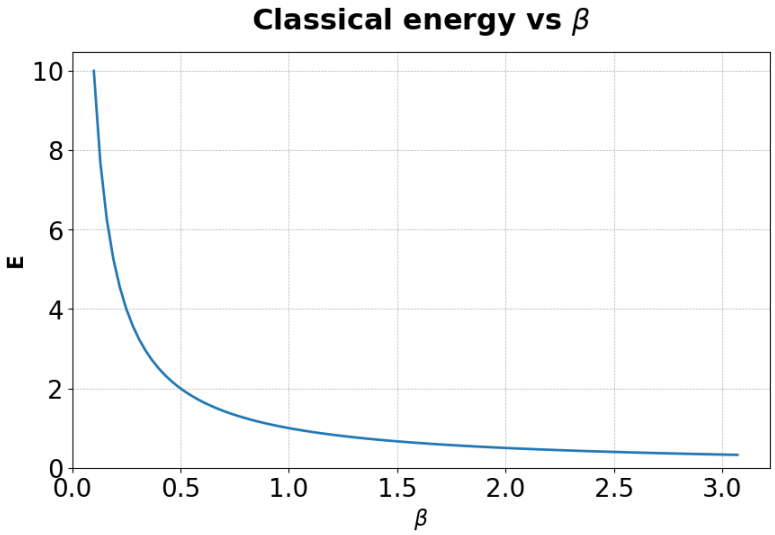

Figure 2.1: Total expectation energy in the classical harmonic oscillator model

In the Monte Carlo simulation, we have to let the system run until it reaches equilibrium, and then run it some more and collect the data for averaging.
For each temperature, we start with the particle centered at $x_0 = 0$ and propose random displacements following:

$$x_1 = x_0 + \Delta$$

These displacements are accepted or rejected using the $M(RT)^2$ criterion with distribution probability:

$$P(x_n) = \frac{1}{Z} e^{-\beta V(x_n)}$$

Then another move is proposed

$$x_{n+1} = x_n + \Delta$$

The process is repeated until the system reaches equilibrium saving for every step energy and acceptance. The choice of Δ is made on an ad hoc basis in such a way as to achieve an acceptance around 50% [Appendix 4.1].
The same procedure is done for multiple temperatures, specifically for $\beta = 0.1 + n \cdot 0.05$, where $n = 0, \ldots, 100$.
Energy and acceptance trends for $N_S = 1000$ steps are shown in Fig. 2.2.

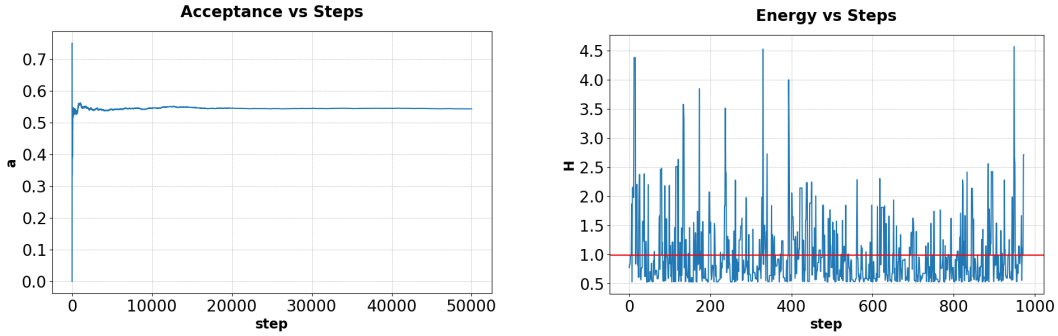

Figure 2.2: Trend of acceptance and energy versus steps for $\beta = 1.0$. Acceptance is usually wanted around 0.5. This rate optimizes the algorithm's performance by ensuring a sufficient acceptance of proposed changes while maintaining effective sampling across the system's states

Since the number of steps to reach equilibrium is unknown and difficult to calculate we calculate the thermalization value as the average of the second half of the set.

$$\bar{H} = \frac{1}{\tilde{N}} \sum_{i=\tilde{N}}^{N_S} H_i$$

$$\sigma_{\bar{H}}^2 = \frac{1}{\tilde{N}^2} \sum_{i=\tilde{N}}^{N_S} (\bar{H} - H_i)^2$$

In the case of $N_S = 1000$ we have:

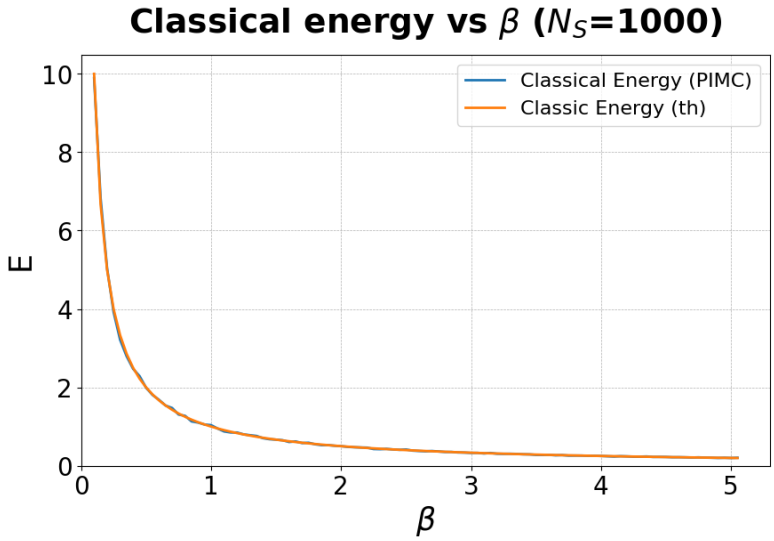

We ran the program for different values of N_S to see how the variance of the data set behaves as a function of it.
We took as values $N_S = 30, 50, 200, 1000$ and these are the results:

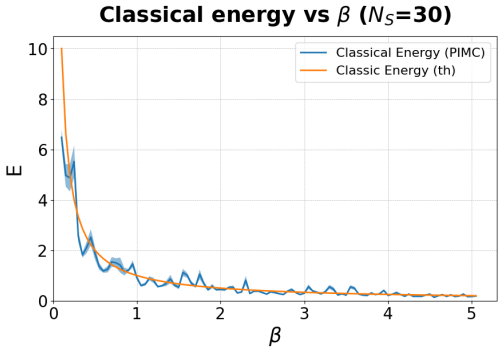

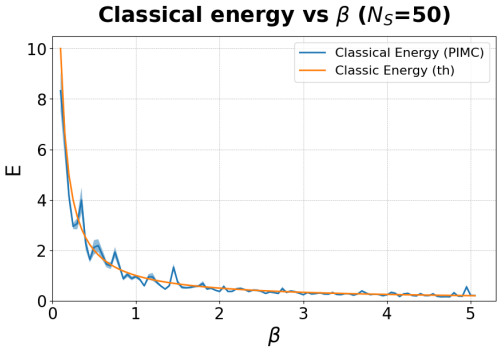

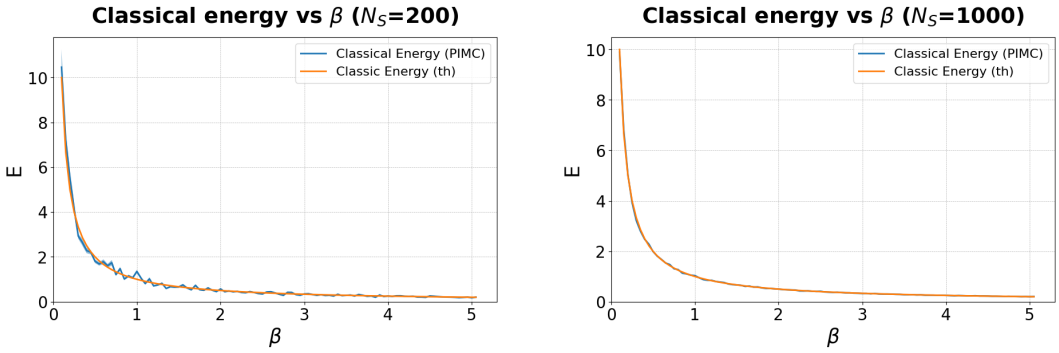

Figure 2.4: From these results we see that in general equilibrium is reached quickly by being a simple one-particle classical system. The standard deviation is lowered with $\tilde{N}$ but it remains smaller than the error made because the number of steps is too low.

2.1.2 Quantum Harmonic Oscillator

In the Hamiltonian of the harmonic oscillator, we replace position and momentum with the operators that characterize them in quantum mechanics

$$\hat{x} = \sqrt{\frac{\hbar}{2m\omega}}(a + a^\dagger)$$

$$\hat{p} = i\sqrt{\frac{\hbar m\omega}{2}}(a^\dagger - a)$$

where $\hat{a}$ and $\hat{a}^\dagger$ are the creation and destruction operators but we do not deal with them for now since by substituting the operators in the Hamiltonian and introducing $\hat{N} = \hat{a}^\dagger\hat{a}$ we arrive at:

$$\hat{H} = \hbar\omega\left(\hat{N} + \frac{1}{2}\right) \tag{2.2}$$

With $\hat{N}$ being the number operator, commutes with the Hamiltonian, and is characterized by the fact that given an eigenstate $|n\rangle$ the eigenvalue is n:

$$\hat{N}|n\rangle = n|n\rangle$$

It is then possible to derive the canonical partition function:

$$Z = \sum_{n=0}^{+\infty} e^{-\beta E_n} = \sum_{n=0}^{+\infty} e^{-\beta\hbar\omega\left(n+\frac{1}{2}\right)} = e^{-\frac{\beta\hbar\omega}{2}} \sum_{n=0}^{+\infty} e^{-\beta\hbar\omega n} =$$
$$= \frac{e^{-\frac{\beta\hbar\omega}{2}}}{1 - e^{-\beta\hbar\omega}} = \frac{1}{e^{\frac{\beta\hbar\omega}{2}} - e^{-\frac{\beta\hbar\omega}{2}}} = \frac{1}{2\sinh\left(\frac{\beta\hbar\omega}{2}\right)}$$

Hence, the internal energy is:

$$E_{qu} = -\frac{\partial \ln(Z)}{\partial\beta} = \frac{\hbar\omega}{2}\left(1 + 2\frac{1}{e^{\beta\hbar\omega} - 1}\right) \tag{2.3}$$

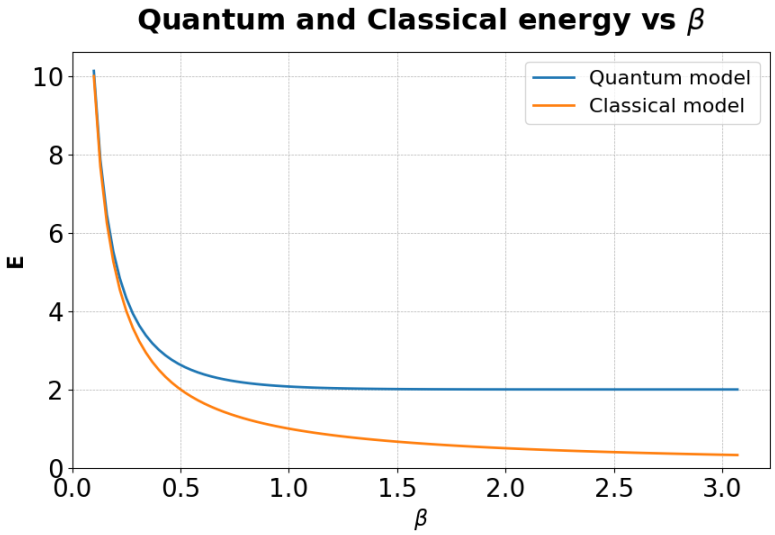

Figure 2.5: Total expectation energy in the quantum model compared with classical harmonic oscillator model for $\delta\omega = 4.0$

Following the path-integral theory presented in the first chapter, we start with M beads in one dimension centered in $R = 0$. As in the classical case we run the program for different values of N_S seeing the trend of energy and the error on it. In particular we set $M = 15$ and $N_S = 10^3, 10^4, 10^5, 10^6$.
The action of the k-th link, following the Eq. 1.5, is:

$$S_k = -\log(\rho(R_{k+1}, R_k; \tau)) = \frac{dN}{2}\log(4\pi\lambda\tau) + \frac{(R_{k+1} - R_k)^2}{4\lambda\tau} + \tau\frac{1}{2}\mu R_k^2 \tag{2.4}$$

The probability distribution in the polymer isomorphism is:

$$P(\{R_0, \ldots, R_M\}) = \frac{e^{-S(\{R_0,\ldots,R_M\})}}{Z} \quad \text{where} \quad S = \sum_{k=1}^{M} S_k \tag{2.5}$$

We initially use as sampling distribution the classical rule of casual shifts within a Δ interval of a randomly chosen bead. So the transition probability between a point $X = \{R_0, \ldots, R_M\}$ to a point $Y = \{R'_0, \ldots, R'_M\}$ is:

$$A(Y|X) = \min\left[1, \frac{P(Y)}{P(X)}\right] = \min\left[1, e^{S(X)-S(Y)}\right] \tag{2.6}$$

The value of Δ in this case is $\Delta = 4\sqrt{\beta/M}$ (the reason for this choice of Δ is explained in Appendix 4.1). For $N_S = 10^4$, considering, for example $\beta = 1.0$, the trends for energy, acceptance, and bead position are shown in the Fig. 2.6.

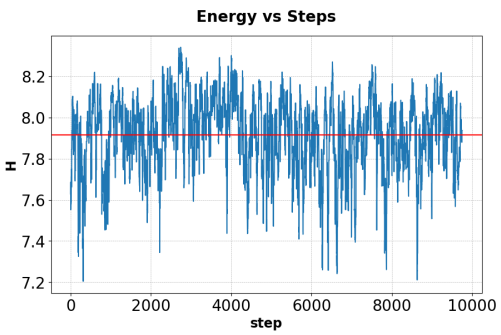

(a). Total energy for each phase. Note that for some steps is negative. Is allowed as long as the average energy is positive average energy is positive.

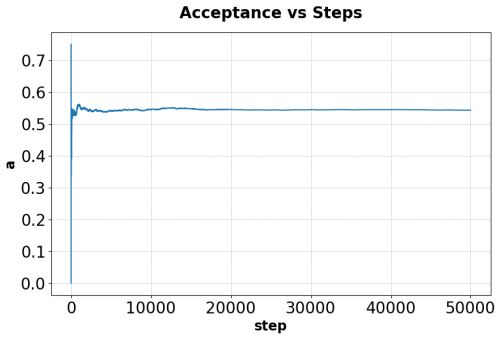

(b). Stable acceptance at 0.5 as desired

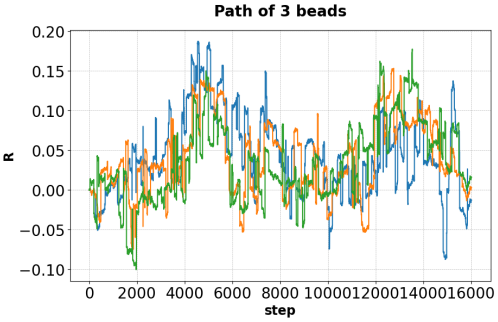

(c). Three random beads of the $M = 15$ used are taken, and the position is relative to the center of mass of the total beads. We took the position relative to the center of mass to see the internal fluctuations in the necklace without being biased by the actual particle in the harmonic potential

Figure 2.6

In primitive approximation the kinetic energy is:

$$\langle \mathcal{T} \rangle = \frac{M}{2\beta} - \frac{mM}{2\hbar^2\beta^2} \sum_i (R_i - R_{i-1})^2 \tag{2.7}$$

the potential is:

$$\langle V \rangle = \frac{1}{2} m\omega^2 \sum_i R_i^2 \tag{2.8}$$

so the expectation energy is given by:

$$E = \langle H \rangle = \langle T \rangle + \langle V \rangle = \frac{M}{2\beta} - \frac{mM}{2\hbar^2\beta^2} \sum_i (R_i - R_{i-1})^2 + \frac{1}{2} m\omega^2 \sum_i R_i^2 \tag{2.9}$$

For $N_S = 1000$ and $\delta\omega = 4.0$ we obtain the graph in Fig. 2.7.

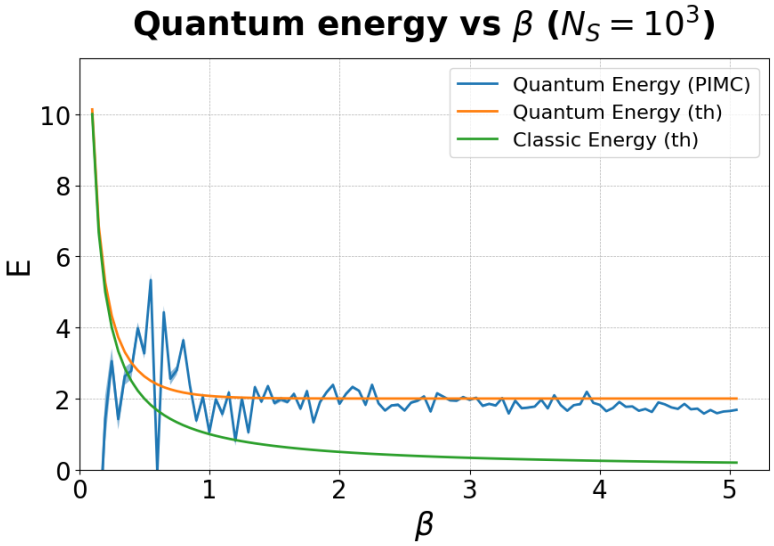

Figure 2.7: It can be seen that that in the quantum case the number of steps we need is much larger than in the classical case

We repeat the same process again for other values of N_S to see for which values we begin to get satisfactory results and to see the standard deviation trend:

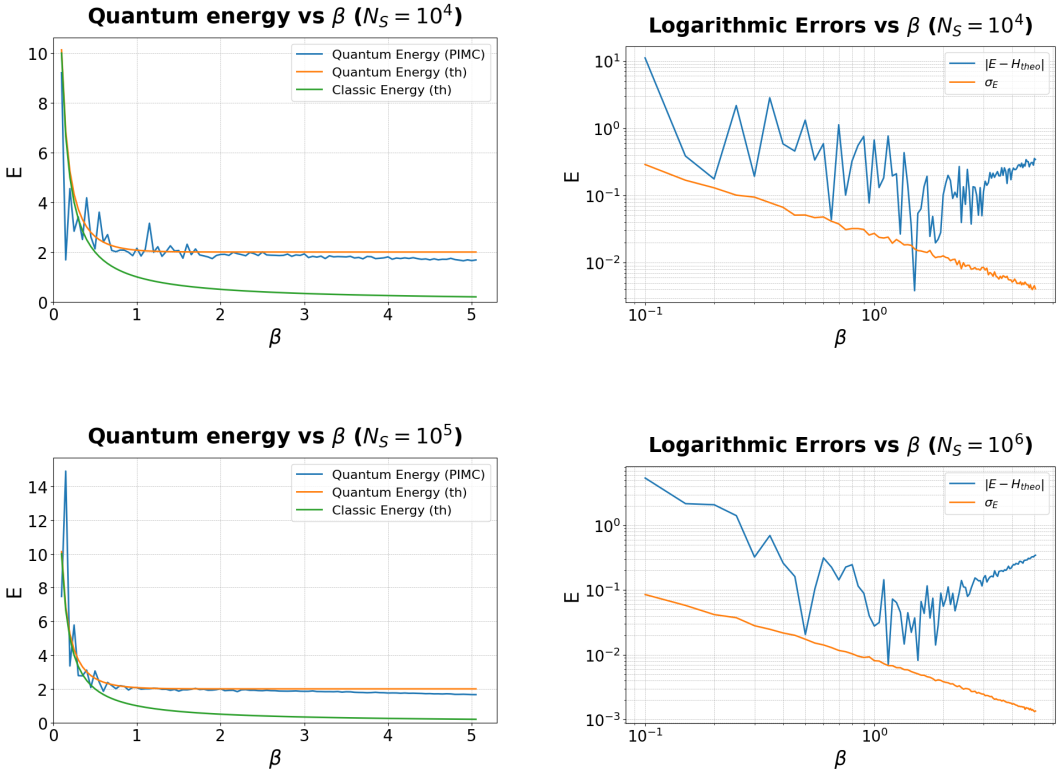

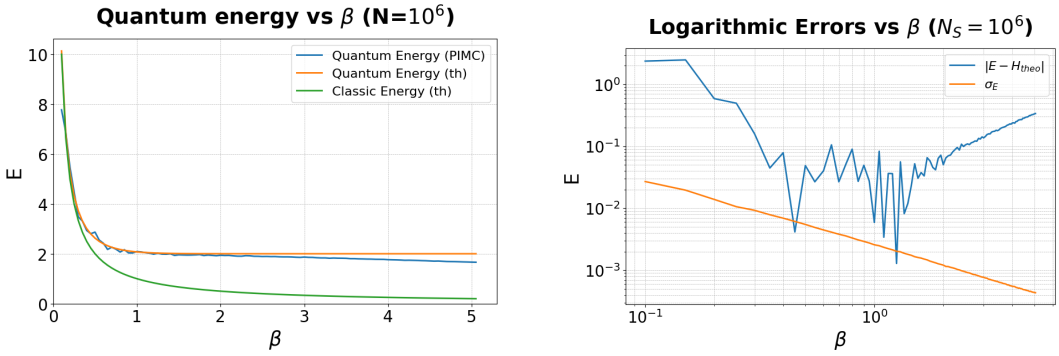

It can be observed that for $N_S > 10^5$ the simulation starts to have a good pattern up to $\beta \simeq 2.0$ After this value we depart from the quantum case approaching the classical case. This is due to the fact that the value of M is good only for

$$M \gg \beta\omega \tag{2.10}$$

and it means that we can simulate the quantum particle using M classical particles only if M is sufficiently large.
The standard deviation always appears very small because as mentioned in the introduction the data obtained from the $M(RT)^2$ algorithm exhibit large autocorrelation. In Appendix 4.2 we see a method to decrease this autocorrelation and in the subsequent graphs we report only the corrected results.
We recompile the simulation program for different values of M with a fixed number of steps $N_S = 5 \times 10^6$. In these cases to see when the system reaches equilibrium we save the energies every 100 steps. We do this mainly to avoid printing an excessive amount of data being that N_S is a large number and also allows us to remove some of the autocorrelations in the first instance.
The number of beads chosen are $M = 5, 15, 50$ and the result is in Fig. 2.11.

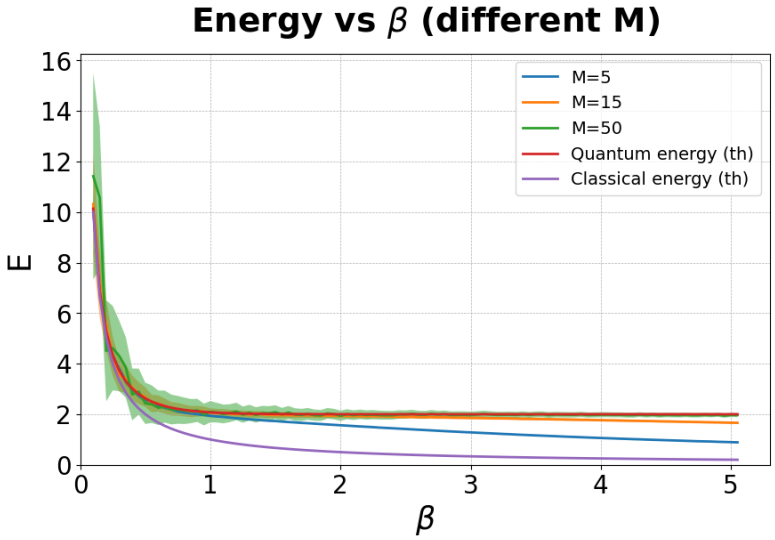

Figure 2.11: Energy for $M = 5, 15, 50$ with $N = 5 \times 10^6$

We note that the Eq. 2.10 is confirmed, however, increasing the value of M results in higher variance for low values of β. In Fig. 2.12 we present the standard deviation (corrected by the autocorrelations) and the error made concerning the expected value.

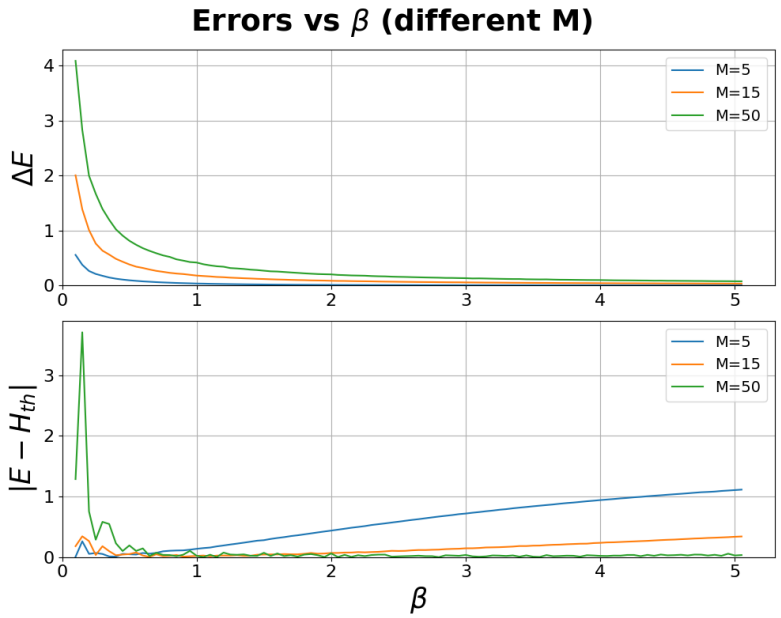

Figure 2.12: Above is the standard deviation of the energies for each temperature corrected by the block method. Below is the error made concerning the expected value.

2.1.3 Smarter Sampling

From the graph in Fig. 2.11 it can be seen that increasing the number of beads results in higher fidelity concerning the harmonic oscillator characteristics. Still because of the sampling distribution chosen, the system converges with greater difficulty even for a large number of steps. This happens especially at high temperatures where the particle is localized in a small area of space and therefore finding the right moves randomly is far from simple. For this reason, we opted to try another type of sampling.
The proposed move is therefore

$$R'_k = \frac{R_{k+1} + R_{k-1}}{2} + \epsilon \quad \text{with} \quad \epsilon \sim \mathcal{N}(0,\, \lambda_\tau) \tag{2.11}$$

and is accepted following

$$A(Y|X) = \min\left[1, e^{V(R_k) - V(R'_k)}\right] \tag{2.12}$$

To compare the two chosen sampling methods, we keep the same values as in the case with $M = 50$ above. So $N_S = 5 \times 10^6$ steps, $M = 50$ beads, $\beta = 0.1 + n0.05$ with $n = 0, \ldots, 100$ and for the harmonic oscillator $\delta\omega = 4.0$.
What we obtain is in Fig. 2.13.

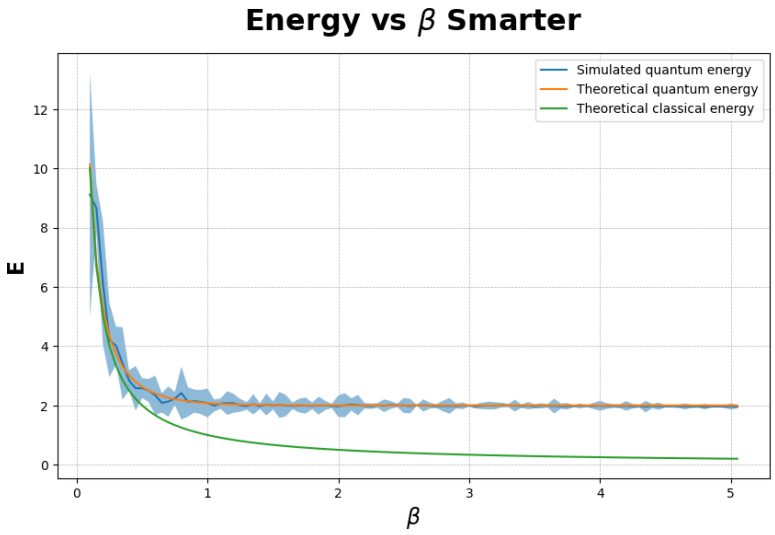

Figure 2.13: Quantum energy for a simulation system with M=50 beads sampling with Brownian bridge method

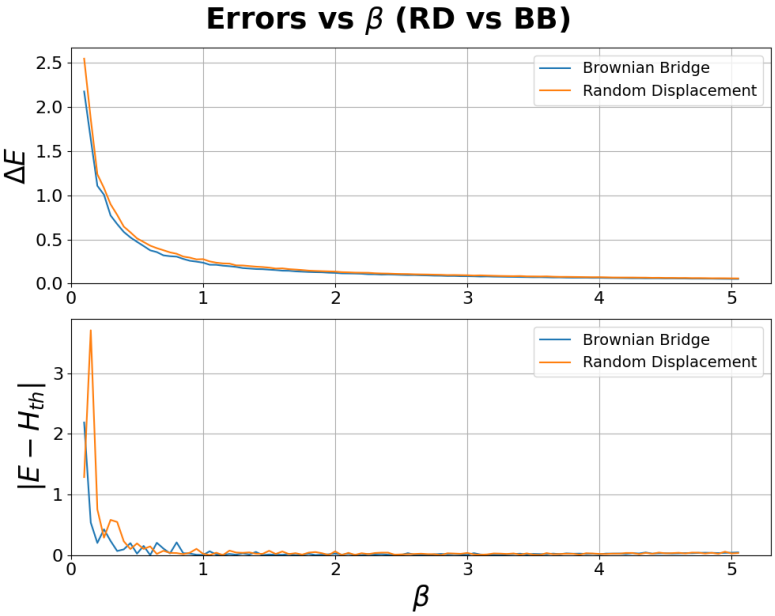

Figure 2.14: Standar deviation and error committed by the two models with different bead-by-bead sampling methods for the same number of steps, number of beads, and oscillator characteristics.

We see that the second type of sampling introduced reports a slight improvement over high temperatures. The real advantage of this approach, however, is the fact that it allows us to write acceptance only as a function of the potential of the displaced bead.

2.2 The anharmonic oscillator

Anharmonic oscillators are physical systems in which the potential energy deviates from the simple quadratic form, often including higher-order terms, and generally do not have exact analytical solutions. Their energy levels are not evenly spaced, and to analyze these

systems, perturbative methods are usually employed to approximate their behavior. We consider a quartic anharmonic oscillator with the potential:

$$V(x) = \frac{1}{2}m\omega^2 x^2 + \lambda\frac{m^2\omega^3}{\hbar}x^4$$

The Hamiltonian can be separated into two terms: the harmonic term and a perturbation term due to the anharmonicity $H = H_0 + H_1$

$$H_0 = \frac{p^2}{2m} + \frac{1}{2}m\omega^2 x^2 = \hbar\omega(n + \frac{1}{2})$$

$$H_1 = \lambda\frac{m^2\omega^3}{\hbar}x^4$$

Remembering the form of the position operator introduced with the harmonic oscillator, it will be

$$H_1 = \lambda\frac{\hbar\omega}{4}(a + a^\dagger)^4$$

in this way, if the anharmonicity is small with respect H_0 we can use the perturbation theory and estimate the eigenvalues and eigenstate of the Hamiltonian.

$$\Delta E_n = \lambda\frac{\hbar\omega}{4}\langle n|(a + a^\dagger)^4|n\rangle$$

knowing that $a|n\rangle = \sqrt{n-1}|n\rangle$ and $a^\dagger|n\rangle = \sqrt{n}|n\rangle$ for the ground state one can obtain:

$$\Delta E_0 = \frac{3}{4}\omega\hbar\lambda \tag{2.13}$$

On the other side in the computational approach we can calculate the action like before and proceed with the PIMC method using the classic rule as the sampling type:

$$S = \sum_{k=1}^{M}\left[\frac{dN}{2}\log\left(\frac{\pi\hbar\tau}{m}\right) + \frac{2m(R_{k+1} - R_k)^2}{4\hbar\tau} + \tau\frac{1}{2}\mu R_k^2 + \tau\lambda R_k^4\right] \tag{2.14}$$

Taking equilibrium values at the same temperature as the harmonic oscillator with $N_S = 5 \times 10^6$ and $\delta\omega = 1.0$ for different values of λ gives the result in the Fig. 2.15.

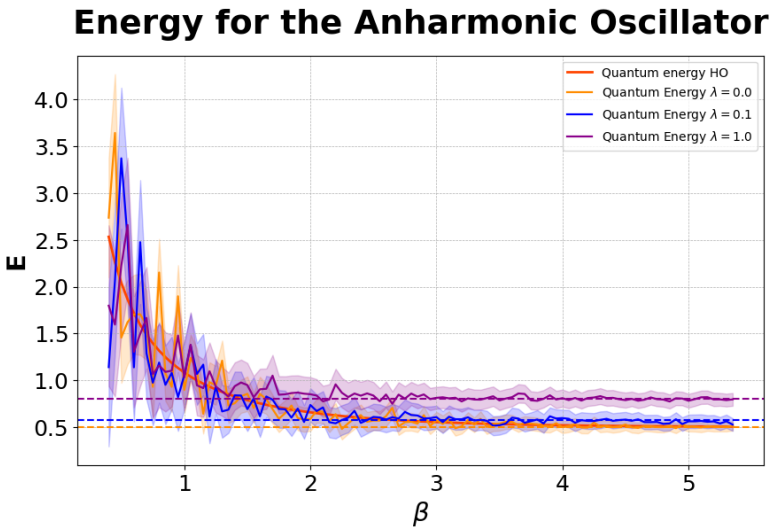

Figure 2.15: Internal Energy for $\lambda = 0.0, 0.1, 1.00$. Ground State values for values smaller than $\lambda = 1$ are calculated by the perturbative method. The case with $\lambda = 1.0$ not being tractable as perturbation H_1 can be found in Ref. [3] and it is 0.8 instead of 1.25 which results in Eq. 2.13

.

From these results, we can say that in the simulation as β grows we get closer and closer to the ground state as expected. For low β we notice large fluctuations.
We propose a solution with smarter sampling:

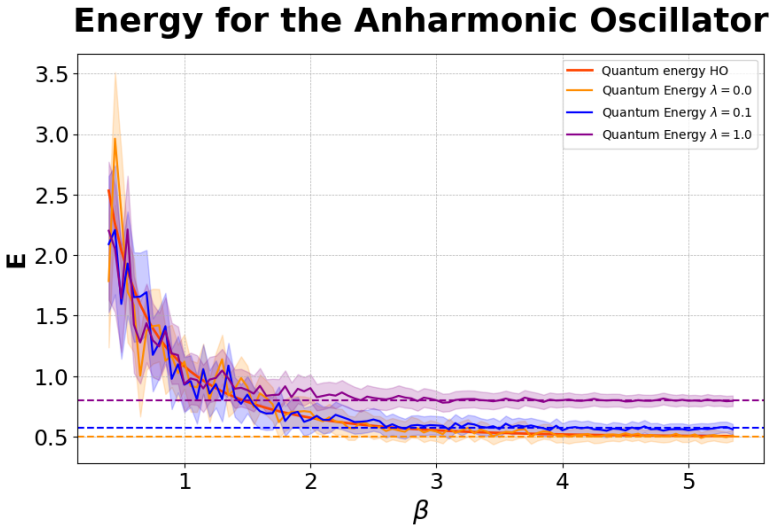

Figure 2.16: Internal Energy for $\lambda = 0.0, 0.1, 1.00$ as before with smarter sampling distribution.

For high β we have the same trend as before while for low β we notice less fluctuation in the lines but we cannot say much since we do not have the exact solution. However, we reiterate that the real gain of this method is that it relies only on the potential of the shifted bead.

Chapter 3

Conclusions

We introduced path integral theory and used it in conjunction with Monte Carlo simulation methods, obtaining the PIMC method. We saw its application for one-dimensional systems. We used two different types of bead-by-bead sampling distributions. These sampling methods can be effective for simple systems. However, when dealing with more complex systems, it is better to abandon them in favor of multilevel methods that, for each step, operate on multiple beads and particles.
We have seen sampling methods such as the classical one that moves the bead at random and the one that uses Brownian bridges, which are the basis of Lévy construction and, more specifically, the bisection method. What we have seen is the basis of PIMC and can be extended to multi-dimensional and multi-particle systems with appropriate accommodations for dimensions.
The results achieved meet the expectations, while the limitations we encoutnered have been properly explained.

Chapter 4

Appendix

4.1 Magnitude of the displacement

Since the polymer extension is proportional to $\sqrt{\beta}$, we try to find a sampling step as a function of β. In particular, we do this once for the classical case and again by fixing $M = 15$. The way the best value is chosen is by running the program by modifying $\Delta = \eta\beta$ for multiple values of β, analyzing the acceptance, and maintaining the value of η which it stabilizes at $a = \frac{\#\text{accepted values}}{\#\text{total samples}} \simeq 0.5$.

β	η_{cl}	η_5	η_{15}	η_{50}
0.06	67.6	7.5	4.35	2.41
0.3	6.0	3.28	1.94	1.07
0.6	2.1	2.15	1.35	0.76
1.0	1.0	1.41	1.05	0.59

Table 4.1: Values of η for different β in the classic system harmonic oscillator and for quantum harmonic oscillator simulated with $M = 15$

Given multiple pairs of $\eta - \beta$ values we can operate by regression and obtain an estimate for $\eta = f(\beta)$. In particular, we study the logarithms of the data found and perform a lien regression to find the law:

$$\ln(\eta) = m\ln(\beta) + q \quad \Rightarrow \quad \eta = \beta^m e^q$$

We then have for each M and for the classical system the value of Δ as a function of β:

$$\Delta_{cl} = \eta_{cl}\beta \simeq \frac{1}{\sqrt{\beta}}$$

$$\Delta_5 = \eta_{15}\beta \simeq \sqrt{\beta}e^{0.05}$$
$$\Delta_{15} = \eta_{15}\beta \simeq \sqrt{\beta}e^{1/2}$$
$$\Delta_{50} = \eta_{50}\beta \simeq \sqrt{\beta}e^{-1/2}$$

we plot $\Delta = \eta\beta$ as a function of beta for different M:

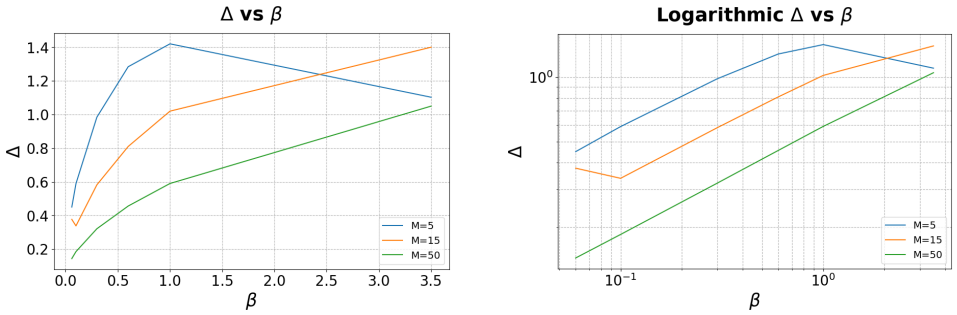

Figure 4.1: Graph and logarithmic plot of the various values of Δ as a function of the variable β alone. It can be seen that by cutting the extremes, i.e. the highest and lowest beta values, the trends are parallel, confirming the fact that $\Delta \propto \beta^{\alpha}$ with $\alpha = 1/2$ found previously

We can see that in general, this value decreases as M increases. Let us then also try to introduce the contribution of M in such a way that we get $\Delta = f(\beta, M)$. Let us pose $\Delta = f(\beta/M)$ assuming that this displacement is of the order of the thermal wavelength $\lambda\tau = \sqrt{\frac{\hbar^2\beta}{2mM}}$.
We plot Δ as a function of the β/M ratio in a single graph and see the trend

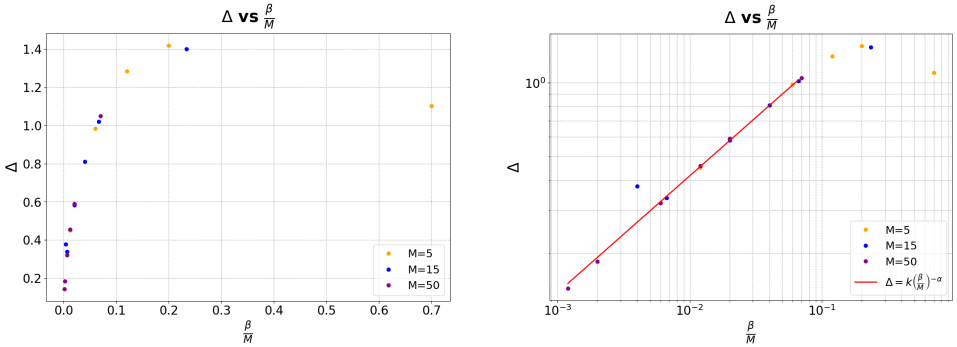

Figure 4.2: Normal and logarithmic graphs. In this case, it can be seen that most of the values follow the same law given by the equation $\Delta = k\left(\frac{\beta}{M}\right)^{m}$. The regression was done by removing the four highest values and the third value because they were considered to be outside the model sought.

The results obtained for the model on the right in Fig. 4.2 show a law of the type:

$$\Delta = k\left(\frac{\beta}{M}\right)^{m} \qquad \text{with} \qquad k = 3.77, m = 0.47$$

We feel entitled to say that for not too-high values of β (where the system is localized in a small part of space), one can use this law to achieve stable acceptance at 0.5 for each β and each M.

4.2 Autoccorelation

Using the $M(RT)^2$ algorithm with Markov Chain, we have to ensure that the elements are independent of each other. In particular, by increasing the number of beads we have that step $n+1$ will be connected to step n being that in this project we use sampled bead by bead and thus move only one bead while the other $M-1$ will be stationary

For every value of β, we subdivide the results of the simulation into blocks of B points each and calculate the average for each block.

$$\langle F \rangle_b = \frac{1}{B} \sum_{i=1}^{B} F_i^{(b)}$$

with $b = 1, \ldots, N_B$ as an index that identifies the block. The total average remains the same:

$$\langle F \rangle = \frac{1}{N} \sum_{i=1}^{N} F_i = \frac{1}{N_B} \sum_{b=1}^{N_B} \langle F \rangle_b$$

while the variance is given by:

$$\sigma^2(\langle F \rangle_b) = \frac{1}{N_B} \sum_{b=1}^{N_B} (\langle F \rangle_b - \langle F \rangle)^2$$

and therefore the error is estimated as:

$$\Delta F(N_B) = \sqrt{\frac{\sigma^2(\langle F \rangle_b)}{N_B}} = \sqrt{\frac{\sigma^2(\langle F \rangle)}{N/B}}$$

For sufficiently large blocks, $B \gg \tau$, the averages in the blocks become uncorrelated and we can thus estimate the correct error:

$$\Delta F(N_B) = \sqrt{\frac{\sigma^2(\langle F \rangle_b)}{N_B}} \xrightarrow{N \gg B \gg \tau} \Delta F(N) = \sqrt{\frac{\sigma^2(F)}{N}(1+\tau)} \tag{4.1}$$

with τ:

$$\tau = \lim_{B \to \infty} \frac{B\sigma^2(\langle F \rangle_b)}{\sigma^2(F)}$$

using the variance of the whole sample.

For the three values of M chosen we have:

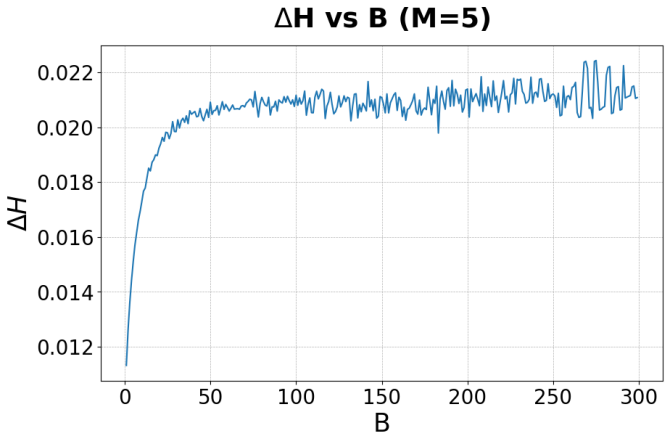

Figure 4.3: Error trend on energy as a function of beta for $M = 5$ beads. It can be seen that a plateau is reached around $B \simeq 50$

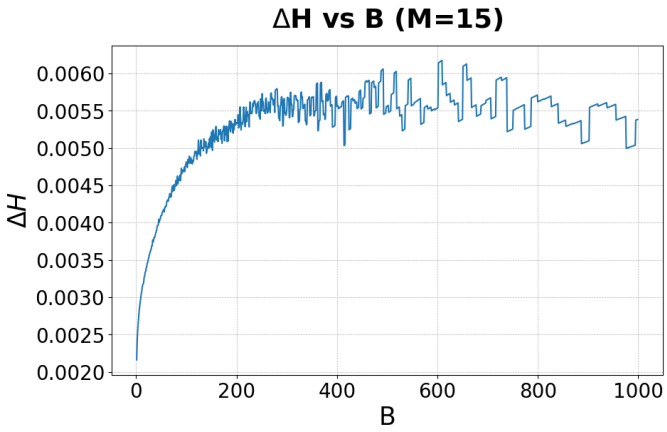

Figure 4.4: Error trend on energy as a function of beta for $M = 5$ beads. It can be seen that a plateau is reached around $B \simeq 250$

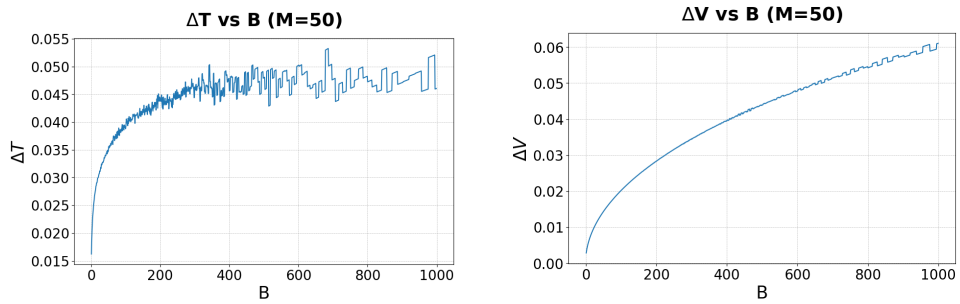

Figure 4.5: Error trend on kinetic and potential energy separately as a function of beta for $M = 50$ beads. Energies were divided because it is difficult for this number of beads to reach the plateau, and we note that the most autocorrelated quantity is potential. One would expect the opposite being that the kinetic energy in primitive approximation is very fluctuating but this result is probably due to the fact that the coupling between beads is less than the characteristic quantities of the harmonic oscillator.

Using Eq. 4.1 it is possible to to correct to a first approximation the variances of the values obtained as follows:

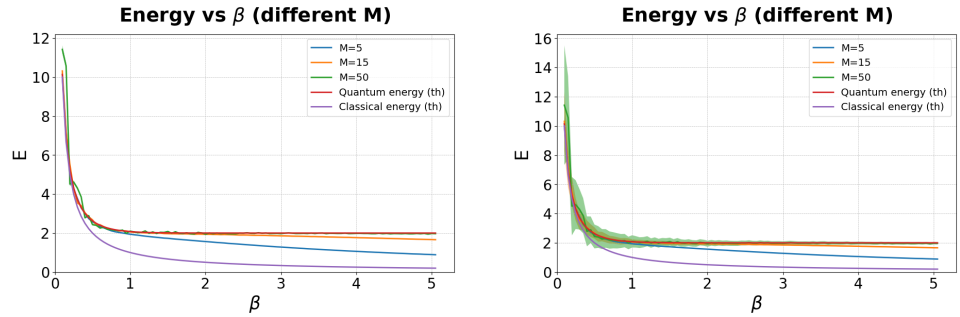

(a). Standard deviation without correction **(b).** Standard deviation after applying the block method

Figure 4.6: Quantum Harmonic Oscillator for $M = 5, 15, 50$. The greatest corrective contribution is seen for M=50 as expected.

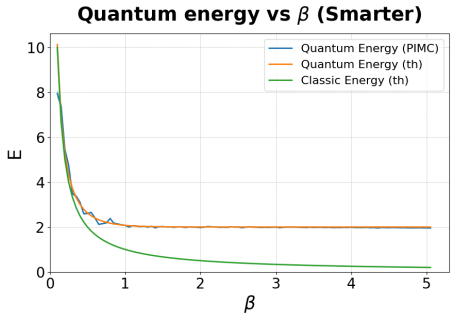

(a). Standard deviation without correction

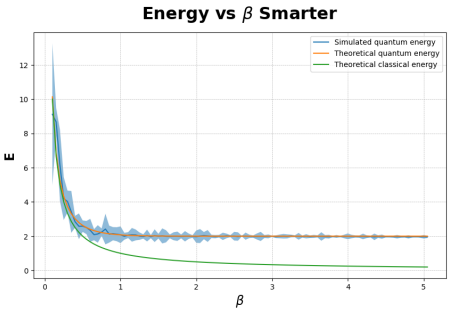

(b). Standard deviation after applying the block method

Figure 4.7: Smarter sampling with $M = 50$

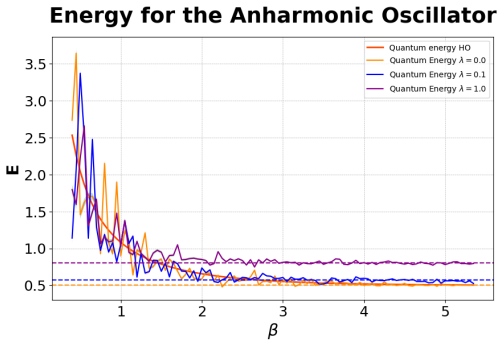

(a). Standard deviation without correction

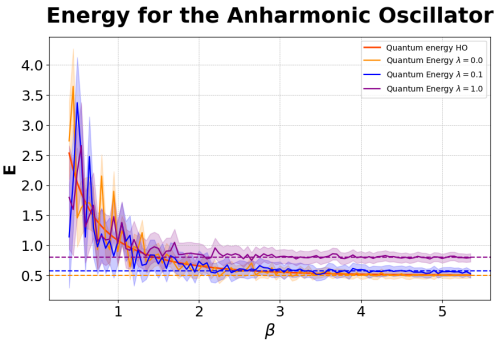

(b). Standard deviation after applying the block method

Figure 4.8: Quantum Harmonic Oscillator for $\lambda = 0, 0.1, 1$.

Bibliography

[1] D. M. Ceperley. Path integrals in the theory of condensed helium. 1995.

[2] Joakim Löfgren. The monte carlo method and quantum path integrals. 2014.

[3] P.R. King D.D. Vvedensky S. Mittal, M.J.E. Westbroek. Path integral monte carlo method for the quantum anharmonic oscillator. 2020.